

# The Experimental and Computational Investigation of the Flow in the Diesel Swirl Chamber

W.Qian, L.Tiqian, L.Detao and Y. Weijia\*

Jiangsu Institute of Technology University  
Zhenjiang  
China

\* Nanjin Hongkong Chang Jiang Co., Ltd.

## ABSTRACT

In this paper, the air flow field in the swirl chamber of a motored diesel engine was measured by a Laser Doppler Anemometry (LDA). The tested diesel engine was S195 diesel engine with a bell type swirl chamber. This study concentrated on the flow fields during the compression stroke. Measurements were made at engine speed of 900r/min. The experiments data was acquired and processed by a quick data acquisition and processing system. Based on the measurements and modified  $k-\epsilon$  turbulence model, a flow numerical model for the bell type swirl chamber of the tested engine was established. To compare the measured data with the calculated results showed that they were well agreed each other.

## INTRODUCTION

The air-motion in the swirl chamber of a diesel engine is one of key factors to control air-oil mixing. Although the study on it has been carried out for several years, the measurement porcceding was limited to mechanical methods and water-simulation [1] [2] without correspondent calculated results. In recent years, new methods and computer technology have been empolyed in studies, but the measurement were conducted in fixed volume model and the results did not denote the real flow. In this paper, the air flow field in the bell type swirl chamber of the S195 diesel engine was measured by LDA. Based on the measurement results and modified  $K-\epsilon$  turbulence model, a numerical model was tested and verified.

## EXPERIMENTAL APPARATUS AND METHODS

The test engine is a reformed model S195 single cylinder bell type swirl chamber diesel engine, with bore 95mm, stroke 100mm, displacement 815cm<sup>3</sup>, swirl chamber volume

25.7cm<sup>2</sup> and compression ratio 19. Two quartz windows are installed on each side of the bell type swirl chamber as the laser beam accesses unchanging volume ratio and compression ratio of the original engine (Fig.1). The measured area is about 80.2 percent of the section of the swirl chamber. the engine is motored via gear box.

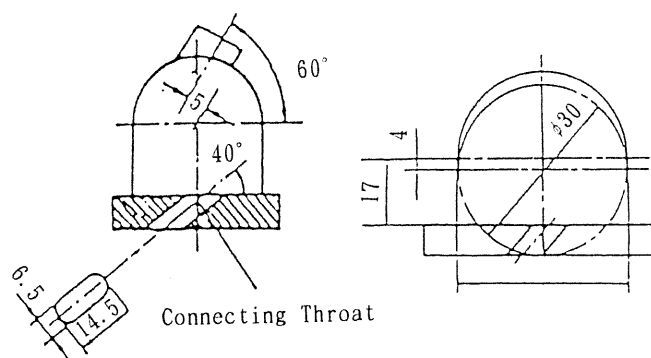


Fig.1 The size of swirl chamber and the measured area

The experimental arrangement consisting of three parts: (1) mechanic system driving the test engine (2) LDA (3) data acquisition and proccession system are shown in Fig.2

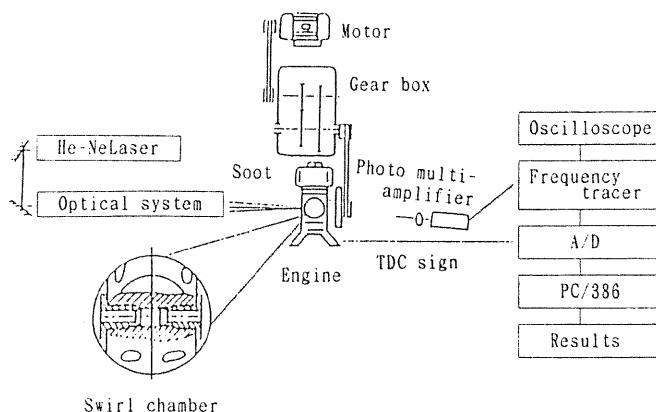


Fig.2 The experimental arrangement

\* Projects of Doctoral Foundation of China

The LDA is a two dimensional differential system. A laser beam is passed through a diffraction fringe rotated in a stable speed and diffracted to  $0, \pm 1, \pm 2 \dots$  order diffraction beams. The  $\pm 1$  order beams go through polarizers seperately and become linear polarized laser beams. Then the 0 and  $\pm 1$  order diffraction beams are focused in the measurment point and interfer each other to form two groups of interference fringes vertical each other with preset frequency shift. This system could measure the two velocity components and judge the flow direction. When a particle suspended in air passes the fringes, it reflects laser lights with Doppler frequencies  $F_d$ . Then  $F_d$  is measured and the velocity component  $V_f$  in vertical direction of the fringes could cal culated by the formula:

$$V_f = \frac{\lambda F_d}{2 \sin(\alpha/2)}$$

where  $\lambda$  is laser light wave length;  $\alpha$  is laser beam inter-section angle.

The LDA system consists of a 25mw He-Ne laser emmiting light with wavelength of 632.8nm, a F500mm launching len and a F300mm receiving Fourier len. The inter-section angle of two beams is  $3^\circ$ . A kind of soot is sprayed into the swirl chamber via air intake as sizing particles. This dued to considering the relation between soot diameter and signal quality. The soot particle size is about  $1.2\mu\text{m}$  and its density into the swirl chamber could be adjusted. The velocity of soot could approximately represents air velocity and could be actually calculated by computer:

$$V_f = 1.342 * 10^{-3} * (127.589 + 0.078778V)$$

where V is mean A / D converting simulating voltage.

## NUMERICAL MODEL

In order to predict air-motion in the bell type swirl chamber, a numerical model of flow in the swirl chamber had been established.

### (1) The Main Hypotheses

(a)The air-motion in the bell type swirl chamber is two dimensional.

(b)Turbulence: A modified K- $\epsilon$  turbulence model is used.

(c)Boundary condition: at the wall surface, the velocity distribution agrees with the 1 / 7 power law.

### (2)Aerodynamic Equations

Continuous equation for cell m is:

$$\frac{\delta \rho_m}{\delta t} + \nabla \cdot (\rho_m u) = \nabla \cdot \left[ \rho D \nabla \left( \frac{\rho_m}{\rho} \right) \right] \quad (1)$$

where  $\rho_m$  is mass density of m;  $\rho$  is total mass density; u is air velocity; D is the diffusivity of m. The momentum equation for the fluid mixture is:

$$\frac{\delta(\rho U)}{\delta t} + \nabla \cdot (\rho u u) = -\frac{1}{\alpha} \rho - A_0 \nabla(2/3 \rho K) + \nabla \cdot \sigma + \rho g \quad (2)$$

where p is air pressure;  $\alpha$  is undimensional value;  $A_0=0$  if the flow is laminal and  $A_0=1$  if the flow is turbulent;  $\sigma$  is the viscous stress tensor given by:

$$\sigma = \mu[\nabla u + (\nabla u)^T] + \lambda \nabla \cdot u Q \quad (3)$$

where Q is the unit dyadic.

The internal energy equation is:

$$\frac{\delta(\rho I)}{\sigma t} + \nabla \cdot (\rho u I) = -\rho \nabla \cdot u + (1 - A_0)\sigma : \nabla u - \nabla \cdot J + A_0 \rho \epsilon \quad (4)$$

where I is the specific internal energy of the fluid (chemical energy exclusive); J is the heat flux vector given by:

$$J = -K \nabla T - \rho D \sum_m h_m \nabla (\rho_m / \rho) \quad (5)$$

where T is the absolute temperature and  $h_m$  is the specific enthalpy of cell m.

The state relations for ideal gas are:

$$p = R_0 T \sum_m (\rho_m / W_m) \quad (6)$$

$$I(T) = \sum_m (\rho_m / \rho) I_m(T) \quad (7)$$

$$C_p(T) = \sum_m (\rho_m / \rho) C_{pm}(T) \quad (8)$$

$$h_m(T) = I_m(T) + R_0 T / W_m \quad (9)$$

where  $I_m(T)$  is the specific internal energy for cell m;  $C_{pm}(T)$  is the specific heat at constant pressure for cell m;  $W_m$  is the molecular weight of cell m;  $R_0$  is the universal gas constant.

The transport coefficients are:

$$\mu = (1.0 - A_0)\rho v_0 + \mu_{air} + A_0 C_\mu k^2 / \epsilon \rho \quad (10)$$

$$\lambda = A_3 \mu \quad (11)$$

$$K = \frac{\mu C_p}{P_r} \quad (12)$$

$$D = \frac{\mu}{\rho S_c} \quad (13)$$

Where  $v_0$  is a constant decided by uniform back-ground turbulent diffusivity;  $\mu_{air} = A_1 T^{3/2} (T+A_2)$ , where  $A_1$  and  $A_2$  are constant,  $A_3 = 2/3$  if the flow is turbulent,  $P_r$  is the Prandtl number and  $S_c$  is the Schmidt number.

This numerical model could be used to calculate the flow in various type swirl chamber. In this paper, only the flow in the bell type swirl chamber during the compression stroke was calculated. The bell type swirl chamber was divided into  $22 * 19$  cells (Fig.3)

## CALCULATED RESULTS

Fig.4 shows the calculated results of the flow in whole bell type swirl chamber with  $40^\circ$  inclination angle of connecting throat.

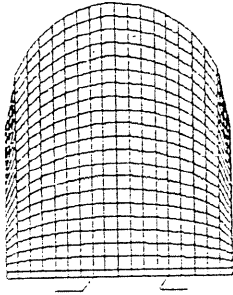


Fig.3 The meshed grid of the swirl chamber

During the compression stroke period, the flow velocity in the swirl chamber goes up with the crank angle increasing. The velocity increases rapidly after about BTDC 130° CA. The velocity in the connecting throat achieves maximum one at BTDC23° CA, and at TDC it drops down to zero. In this working period the flow in the bell type swirl chamber center is more powerful than that in the other area. There is a flow detention area in the up-stream side

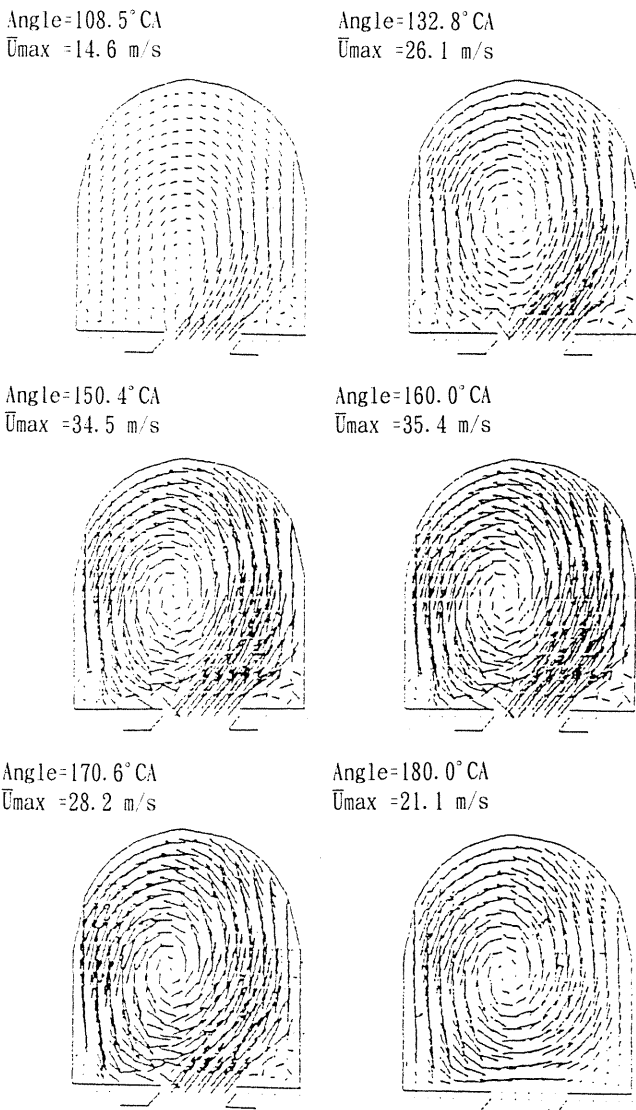


Fig.4 The calculated results

near the wall due to the friction between the air and the wall. In addition the position of vortex core in the swirl chamber moves towards the left-below gradually with crank angle rising from BTDC100° CA to TDC and it is under the center of the swirl chamber at last. As shown in Fig.4, there are two subvortex at the corner of the bell type swirl chamber. This agrees with the results of water-simulation [2].

ANALYSIS OF RESULTS

Fig.5 shows that the velocity in point 1 and point 2 locates at  $r/r_0 = 0.7$  (where  $r_0$  is radius of the swirl chamber) of the bell type swirl chamber change with the crank angle. There the actual line denotes the measured results and the dotted line denotes the calculated results. Two curves have the same shape and nearly same value. The maximum velocity in point 1 occurs at BTDC23° CA (the calculated value  $U_{max}$  is 38.3m/s and the measured value  $U'_{max}$  is 35.4m/s). In point 2 the maximum velocity occurs at BTDC10° CA (the calculated value  $U_{2max}$  is 21.2m/s and the measured value  $U'_{2max}$  is 18.6m/s)

Fig.6 shows the measured and calculated velocity  $U$  change along the  $r/r_0$  at BTDC20° CA and at TDC. The maximum velocity occurs between  $r/r_0 = 0.7$  and 0.9. When the crank angle increases from BTDC20° CA to TDC, the maximum velocity position moves towards the center of the chamber. Comparing the measured results with calculated ones in Fig.6a and Fig.6b, the two results show fairly good agreement.

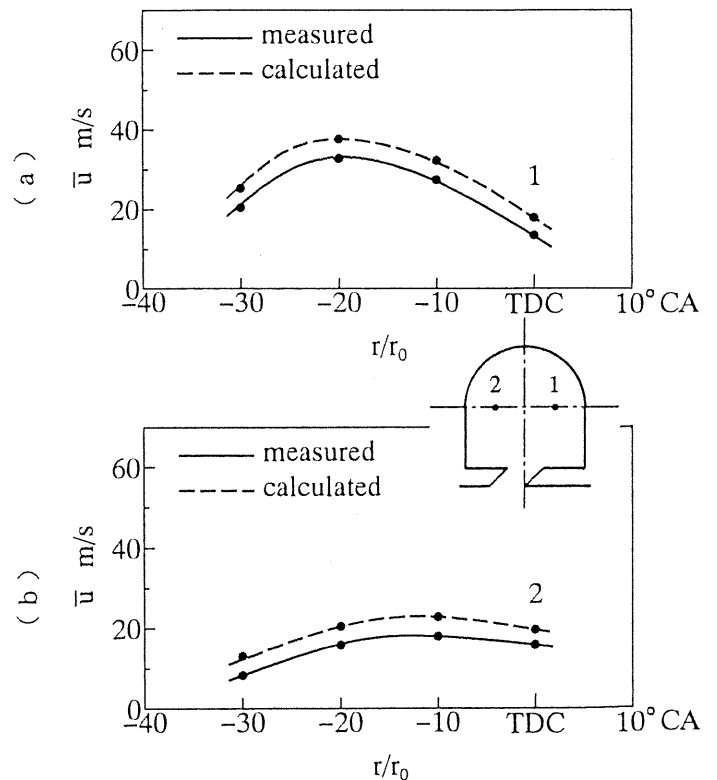


Fig.5 The velocity of flow changes with crank angle

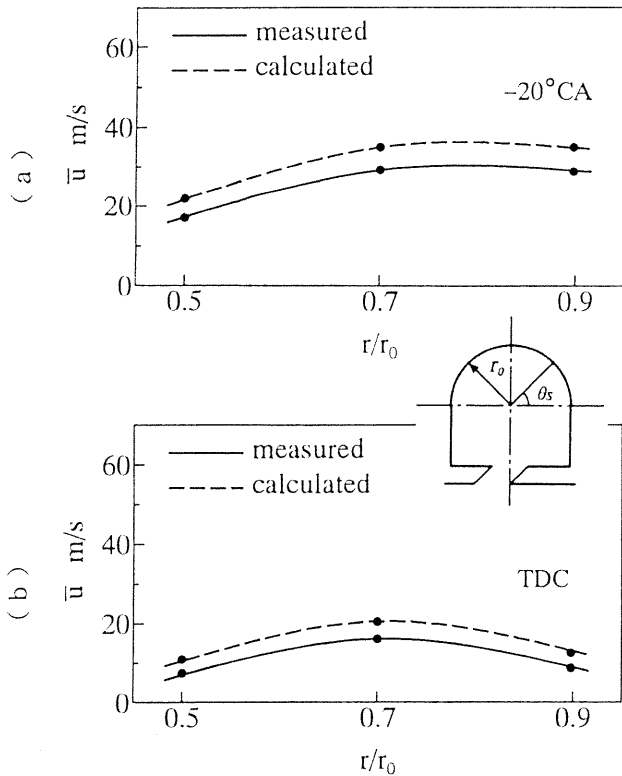


Fig.6 The velocity changes with  $r/r_0$

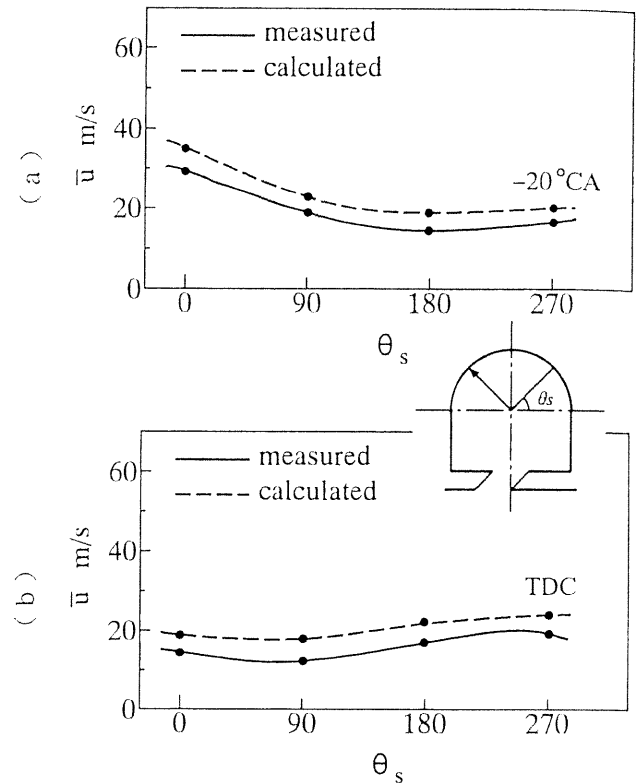


Fig.7 The distribution of the flow with  $\theta_s$

Fig.7 shows the distribution of velocity along  $r/r_0=0.7$  circular in the bell type swirl chamber at TDC and at BTDC20°C A. The angle  $\theta_s$  dominates the position. The mean velocity achieves maximum when  $\theta_s=0$  at BTDC20°C A. The measured  $U_{\max}$  is 33.5m/s and the calculated  $U_{\max}$  is 29.8m/s. When  $\theta_s=0$  the concerned point locates near the connecting throat and is directly influenced by the flow through the throat from the main chamber, especially at BTDC20°C A. When  $\theta_s$  goes up to 90°,  $U$  achieves its low limit and then keeps constant. At TDC  $U$  keeps a steady value because the air velocity in the connecting throat is nearly zero, shown in Fig.7b clearly.

## CONCLUSIONS

(1) In compression process, the tangential velocities in the bell type swirl chamber vary with the crank angle. The velocity in the upstream side goes up with rising of the crank angle. At BTDC23° the velocity gets maximum value. In the downstream side velocities nearly keep constant after BTDC20° and is lower than in upstream side. There are two subvertexes in the corners of the chamber.

(2) In compression process, there are strong vortex motion. In the half compression period, it is a quasi-solid vortex, then changes to quasisolid vertex in the end of the compression period. The vertex core is located near the chamber center at the beginning and in the middle of the compression stroke, then moves down left and at TDC it reaches the down-center of the chamber.

## NOMENCLATURE

- $\lambda$ —laser light wave length, mm
- $\alpha$ —laser beam intersection angle, deg
- $F_d$ —Laser Doppler frequency, Hz
- $V_f$ —the velocity of soot, m/s
- $V$ —mean A/D converting simulating voltage, V
- $\rho_m$ —mass density of m, kg/m<sup>3</sup>
- $\rho$ —total mass density, kg/m<sup>3</sup>
- $U$ —air velocity, m/s
- $D$ —the diffusivity, m<sup>2</sup>/s
- $P$ —pressure, N/m
- $\sigma$ —the viscous stress tensor
- $Q$ —the unit dyadic
- $I$ —the specific internal energy, J
- $J$ —the heat flux vector
- $T$ —the absolute temperature, K
- $h_m$ —the specific enthalpy of cell m, KJ/kg·k
- $I_m(T)$ —the specific internal energy for cell m, kJ/kg·K
- $C_{pm}(T)$ —the specific heat at constant pressure for cell m, kJ/kg·K
- $W_m$ —the molecular weight of cell m
- $R_0$ —the universal gas constant
- $v_0$ —constant
- $\mu_{air}$ —diffusivity of the molecular, m<sup>2</sup>/s
- $A_0, A_1, A_2, A_3$ —constant of the model
- $P_r$ —the Prandtl number
- $S_c$ —the Schmidt number

$r$ —radius coordinate  
 $r_0$ —radius, mm  
 $U_{\max}$ —the maximum flow velocity, m / s  
 $\theta_3$ —angle, deg  
 $\nabla$ —Hamilton operator

Subscrip

air—air flow  
 $\sum$ —total  
 m—cell m

REFERENCES

- 1 H. P. Ricardo, "The High Internal Combustion Engine", London, Blakie And Sons, 1953
- 2 Detao Li, Bemdean V., "Study on Air Movement in Separate Swirl Chamber by Means of a Bidimensional Dynamic Liquid Mode", Rev. Rom Sci. Tech. Mec. appl. 1984
- 3 Gen'ichi KOMATSU, Makoto IKEGAMI, "Numerical Simulation of Air Motion in the Swirl Chamber of Diesel Engines", Proceeding of the 5th Internal Combustion Engine Symp. of Japan, 86-0693A, P1480
- 4 Noboru Miyamoto etl. "Air Flow Analysis in Swirl Chamber with Hot-wire Anemometry", Proceeding of the JSME Annual meeting, No.45, 1990, P9
- 5 Wu Shanmou etl, "The Investigation of Swirl and Turbulence in Diesel Swirl Chamber", Transaction of CSICE, vol.8, No.3 P27 1990